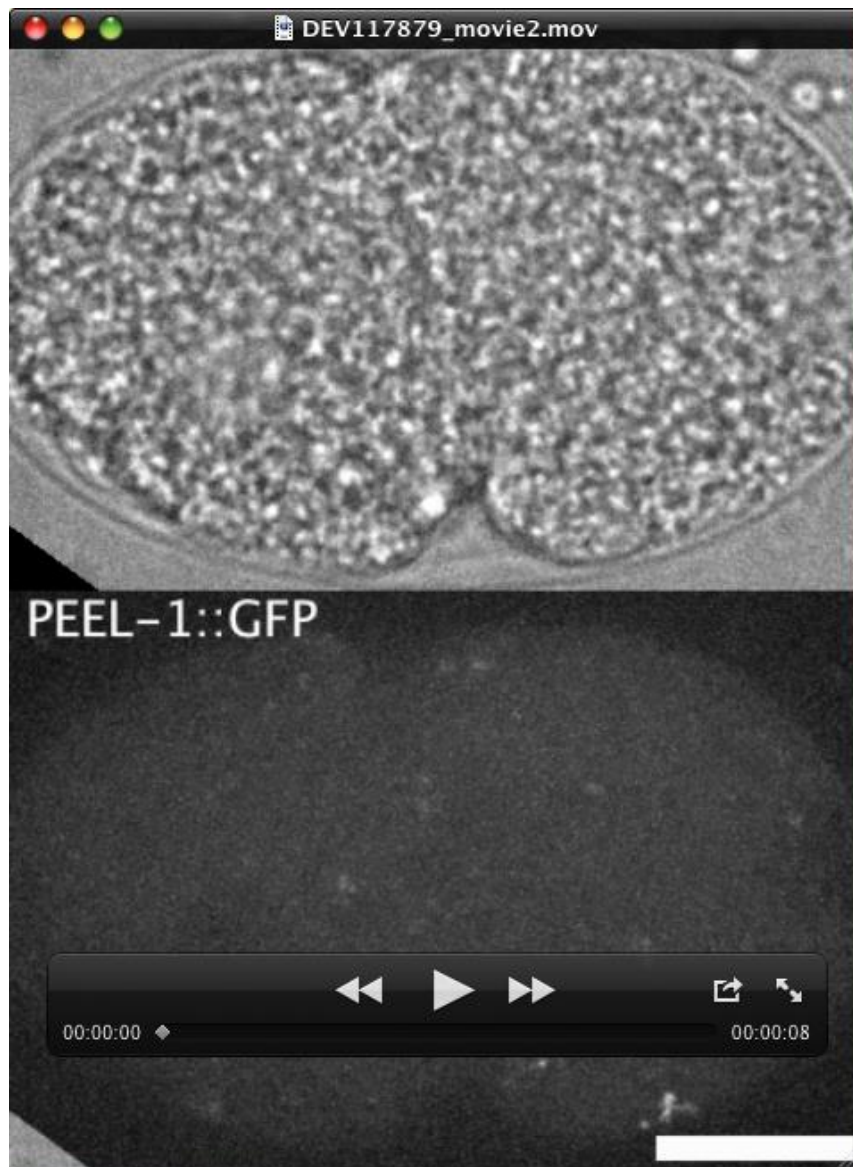**Movie 1:** Sperm mitochondria follow centrosomes dynamics in newly fertilized *C. elegans* embryo Time-lapse recording showing the dynamics of mitotracker labeled sperm-mitochondria (CMXRos, green) in a wild-type embryo. Maximal-intensity Z-projections of images captured every minute with a spinning disk microscope are shown overlaid with single plane DIC images. Scale bar =10μm.

Movie 2: Membranous organelles follow centrosomes dynamics in newly fertilized *C. elegans* embryo

Time-lapse recording showing the dynamics of membranous organelles (MO, gray) in an embryo expressing PEEL-1::GFP. Maximal-intensity Z-projections of images captured every minute with a spinning disk microscope are shown. Scale bar =10μm.

Movie 3: GFP::LGG-2 follows centrosomes dynamics in newly fertilized *C. elegans* embryo

Time-lapse recording showing the dynamics of GFP::LGG-2 (gray) in a 1-cell stage embryo. Maximal-intensity Z-projections of images captured every 30 seconds with a spinning disk microscope are shown. Scale bar =10μm.
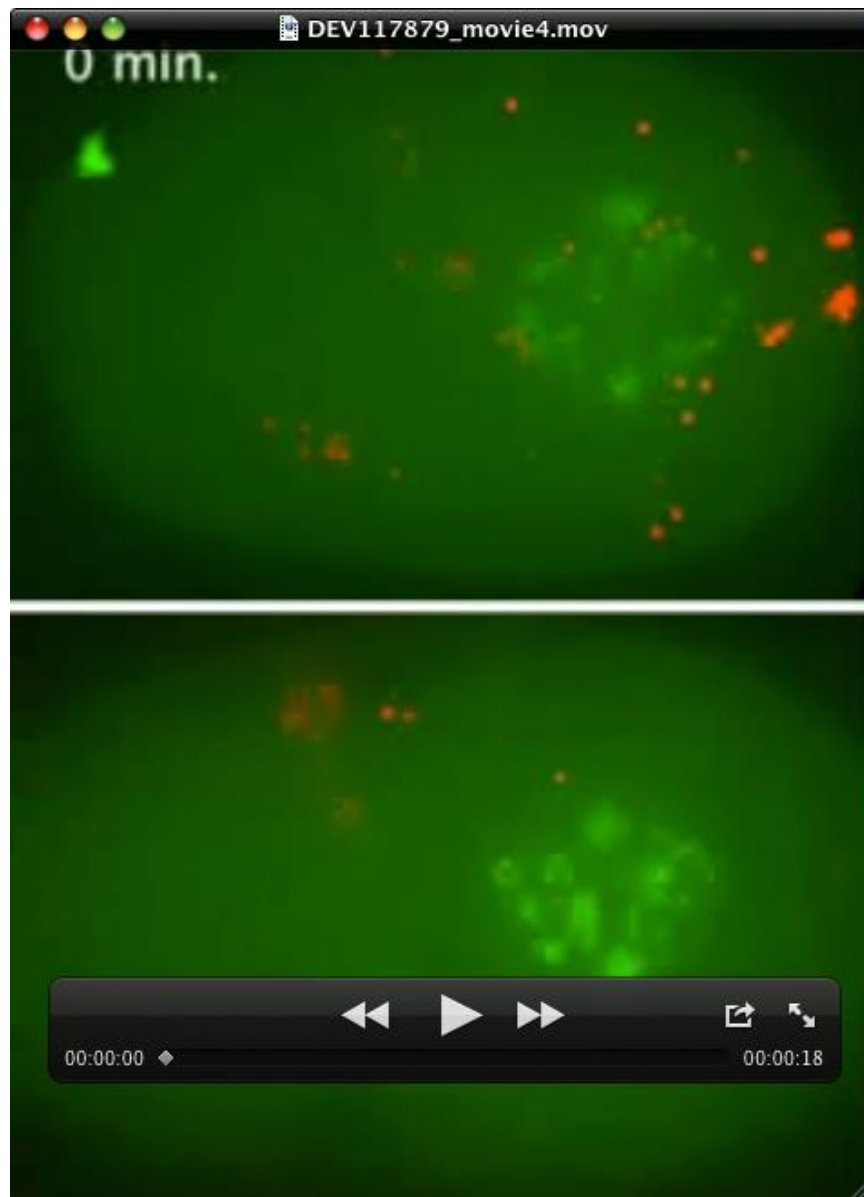
Movie 4: The spatial distribution of sperm mitochondria depends on MTOC and microtubules dynamics during the first embryonic divisions

Time-lapse recordings of wild-type (top) and *lgg-2(tm5755)* (bottom) embryos expressing GFP::ß-Tubulin;GFP::Histone (green) showing the distribution of sperm mitochondria (red). Maximal-intensity Z-projections of images captured every minute with a spinning disk microscope are shown. A Z-stack showing the cortical localization of the mitochondria in the 2-cell stage *lgg-2(tm5755)* embryo is shown at the end.
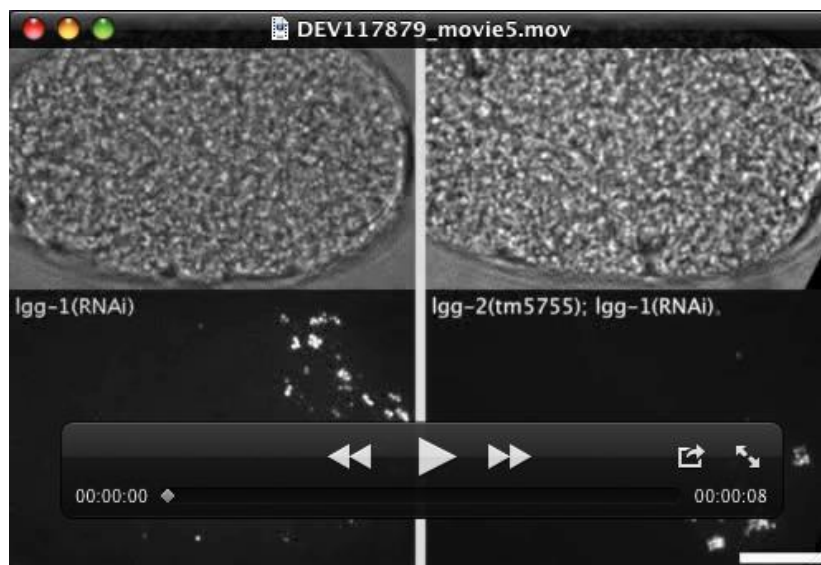
Movie 5: Sperm mitochondria are scattered upon LGG-1 RNAi depletion in both wild-type and *lgg-2(tm5755)* backgrounds

Time-lapse recordings showing the dynamics of mitotracker labeled sperm-mitochondria (CMXRos, gray) upon LGG-1 RNAi depletion in wild-type (left panels) and *lgg-2(tm5755)* (right panels) embryos. Maximal-intensity Z-projections of images captured every minute with a spinning disk microscope are shown. Scale bar =10μm.

Movie 6: Sperm mitochondria are distributed away from the centrosomes in absence of Dynein Heavy chain (DHC-1) during the first embryonic divisions

Time-lapse recording of a *dhc-1(RNAi)* embryo expressing GFP::γ-Tubulin (green) showing the distribution of sperm mitochondria (red). Maximal-intensity Z-projections of fluorescence images overlaid with single plane DIC images captured every minute with a spinning disk microscope are shown. Scale bar =10μm.

Movie 7: The expression of GFP::LGG-1 affects the dispersion of allophagosomes in DHC-1 depleted embryos during the first embryonic divisions

Time-lapse recording of a *dhc-1(RNAi)* embryo expressing GFP::LGG-1 (green) showing the clustering of allophagosomes (green). Maximal-intensity Z-projections of fluorescence images overlaid with single plane DIC images captured every minute with a spinning disk microscope are shown.
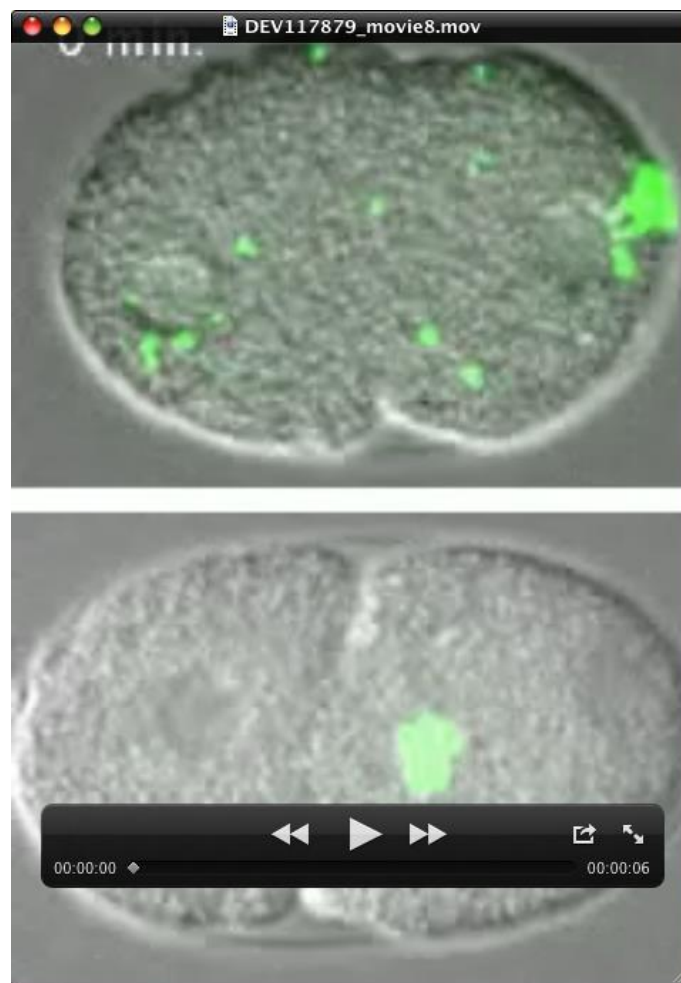
Movie 8: The expression of GFP::LGG-1 affects the dispersion of allophagosomes but not the LGG-2 dependent retrograde transport toward centrosomes

Time-lapse recordings of a wild-type (upper panel) and *lgg-2(tm5755)* (lower panel) embryos expressing GFP::LGG-1 (green) showing the clustering of allophagosomes (green). Maximal-intensity Z-projections of fluorescence images overlaid with single plane DIC images captured every minute with a spinning disk microscope are shown.
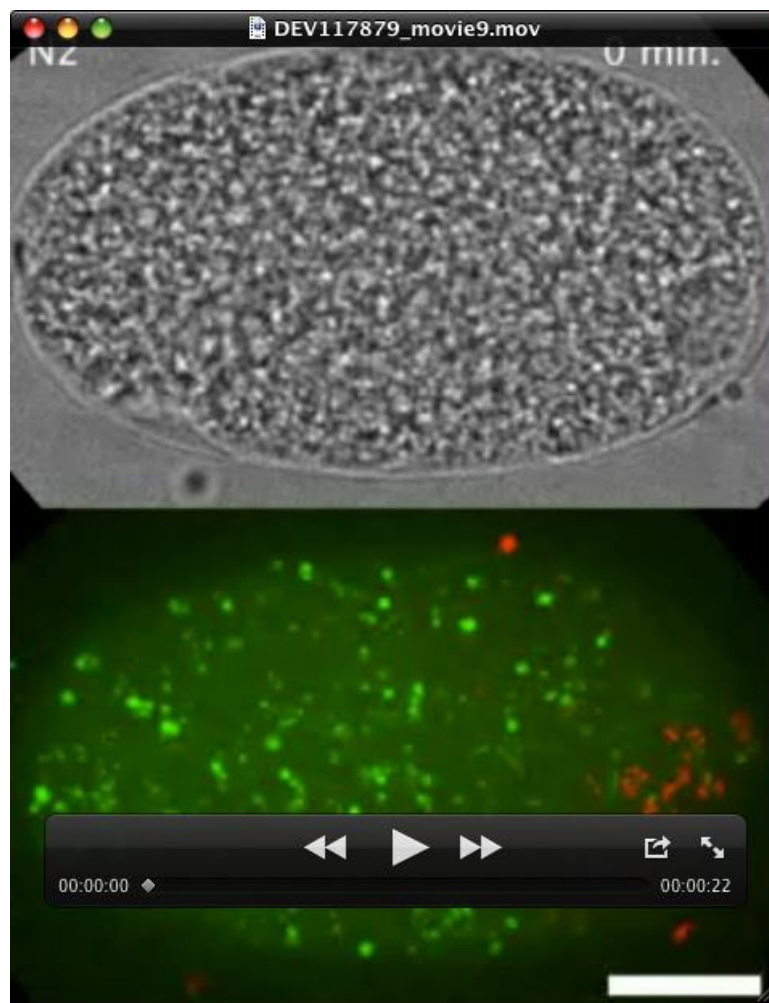
Movie 9: Analysis of acidic compartments and sperm mitochondria dynamics in newly fertilized *C. elegans* embryo

Time-lapse recording of a wild-type embryo showing lysotracker labeled acidic compartments (DND-26, green) and mitotracker labeled sperm-mitochondria (CMXRos, red). Maximal-intensity Z-projections of images captured every minute with a spinning disk microscope are shown. Scale bar =10μm.
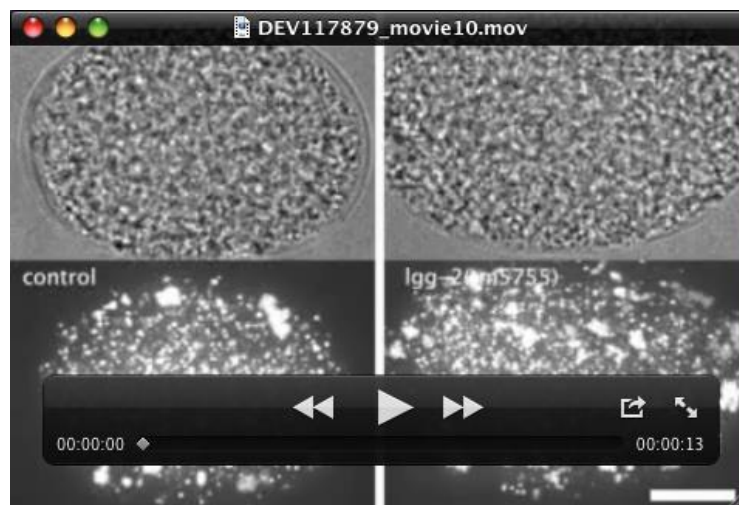
Movie 10: The lysosomal marker NUC-1::mCHERRY is enriched in the pericentrosomal area of newly fertilized *C. elegans* embryo in wild-type and *lgg-2(tm5755)* embryos

Time-lapse recordings of wild-type (control, left panels) and *lgg-2(tm5755)* (right panels) embryos expressing the mCHERRY-tagged lysosomal nuclease (lower panels) showing the distribution of lysosomes during the first embryonic divisions in *C. elegans*. Maximal-intensity Z-projections of images captured every minute with a spinning disk microscope are shown. Scale bar =10μm.

Movie 11: The lysosomal marker LMP-1 is enriched in the pericentrosomal area of newly fertilized *C. elegans* embryo

Movie showing the Z-planes from stacks of immunofluorescence images of wild-type (N2, left panels) and *lgg-2*(*tm5755*) embryos (right panels) at pronuclei rotation stage, stained for LMP-1(green), and DNA (blue) captured using a spinning disk microscope. Z-step between individual images is 0.4µm. Scale bars =10µm.
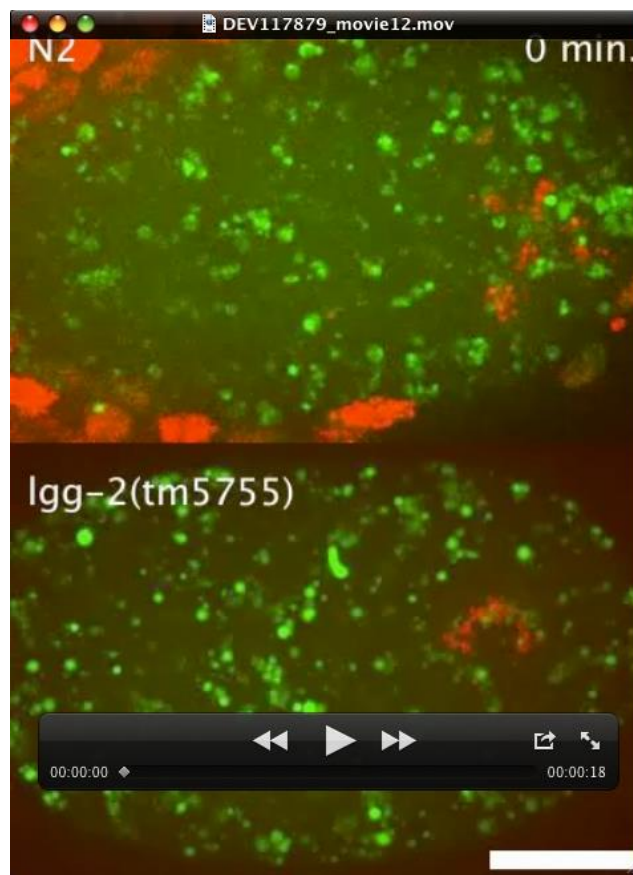
Movie 12: Sperm mitochondria remain away from pericentrosomal acidic compartments in absence of LGG-2

Time-lapse recordings of *lgg-2(tm5755)* (lower panel) compared to wild-type (N2, upper panel) embryos showing lysotracker labeled acidic compartments (green) and mitotracker labeled sperm-mitochondria (red). Maximal-intensity Z-projections of stack of images captured every minute with a spinning disk microscope are shown. Scale bar =10μm.
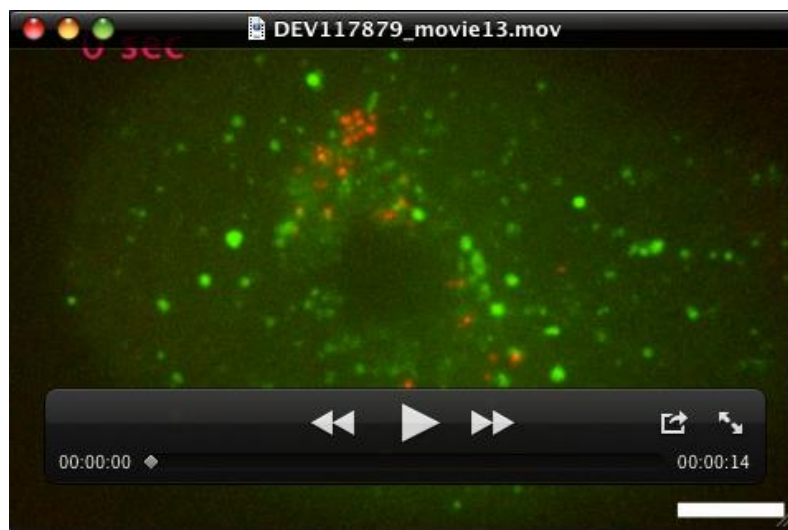
Movie 13: Sperm mitochondria migrating centripetally toward the pericentrosomal area are not in an acidic compartment

Time-lapse recording of wild-type (N2) embryo at pronuclei rotation showing lysotracker labeled acidic compartments (arrow head, green) and mitotracker labeled sperm-mitochondria (arrow head, red) motility toward the centrosome. Maximal-intensity Z-projections of stacks of images captured every 5 seconds with a spinning disk microscope are shown. Scale bar =10µm.
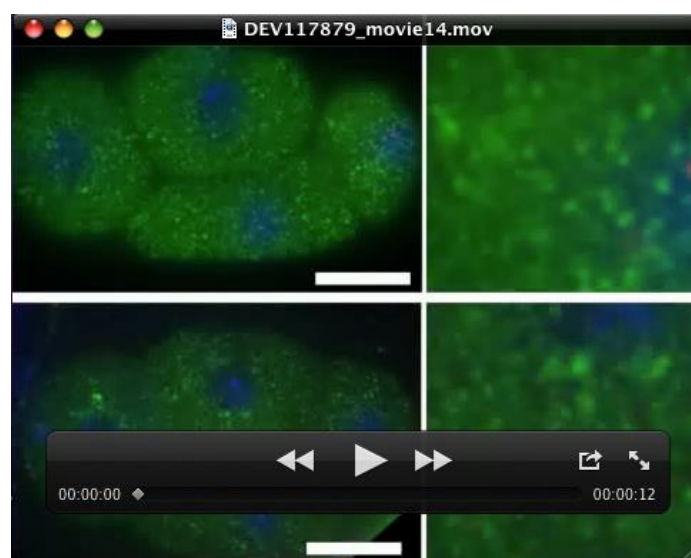
Movie 14: Clustered allophagy structures containing sperm organelles are RAB-7 positive in the absence of LGG-2

Movie showing the Z-planes of a stack of immunofluorescence confocal images of 4-cell stage *lgg-2*(*tm5755*) embryos showing mitotracker labeled sperm-mitochondria (red, upper panels), MO (red, lower panels), RAB-7 (green) and DNA (blue). 4-fold magnified views of the clustered substrates (red) and associated RAB-7 (green) are shown on the right. Z-step between individual images is 0.4μm. Scale bar =10μm.
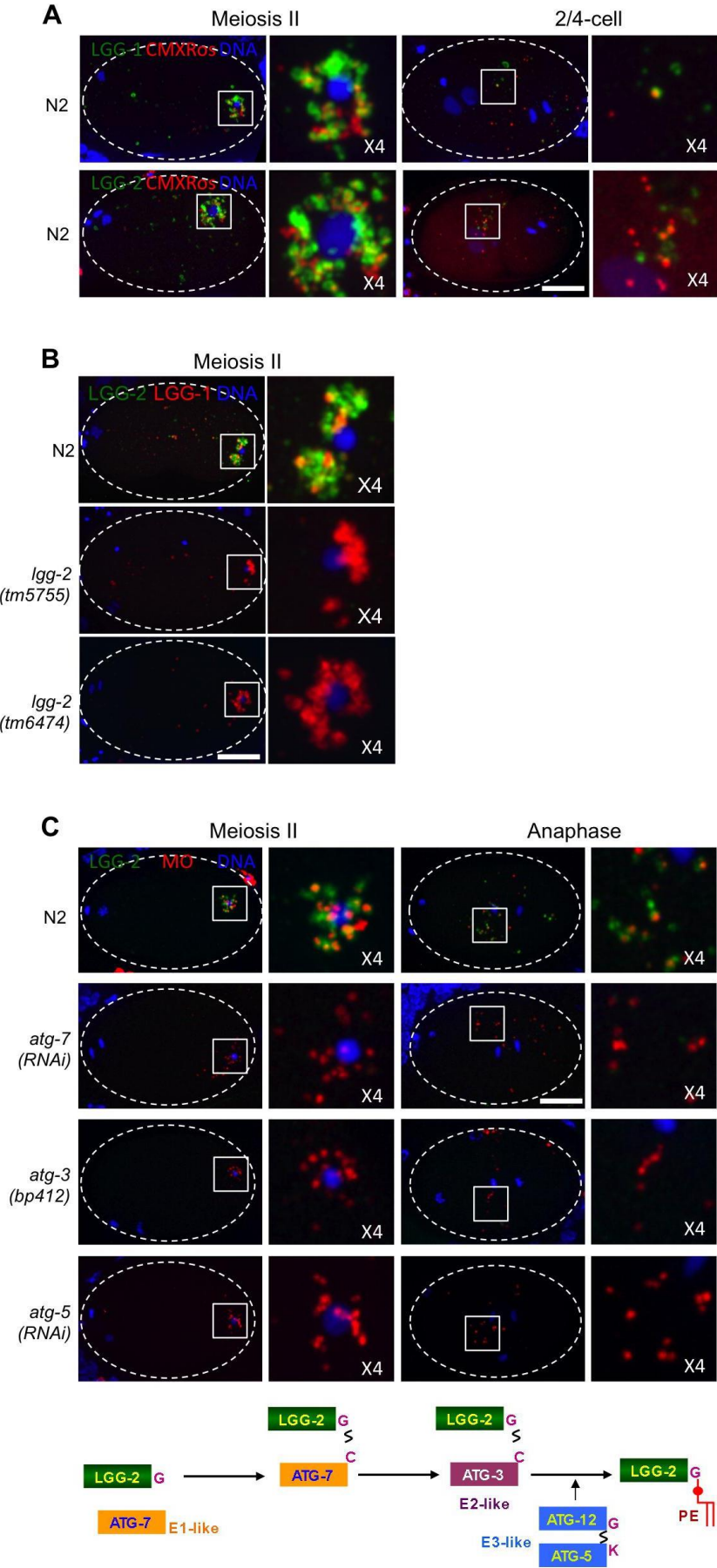
Figure S1: LGG-1 and LGG-2 proteins are both recruited autonomously around sperm inherited mitochondria during meiosis II

A- Maximum intensity Z-projections (MIP) of immunofluorescence images of wild-type (N2) embryos stained for sperm-mitochondria (CMXRos, red), DNA (blue) and LGG-1 (green, upper panels) or LGG-2 (green, lower panels). B- MIP of confocal images of wild-type (N2), *lgg-2(tm5755)* and *lgg-2(tm6474)* embryos stained for LGG-1 (red), LGG-2 (green) and DNA (blue). C-schematic representation of the steps of the ubiquitin-like conjugation pathway in autophagy (bottom) and MIP of confocal images of wild-type (N2), *atg-7(RNAi), atg-3(bp412)* and *atg-5(RNAi)* embryos stained for LGG-2 (green), MO (red) and DNA (blue). On the right of each image are 4-fold magnified views of the highlighted areas. Dotted lines outline the embryos. Scale bars =10μm.

A
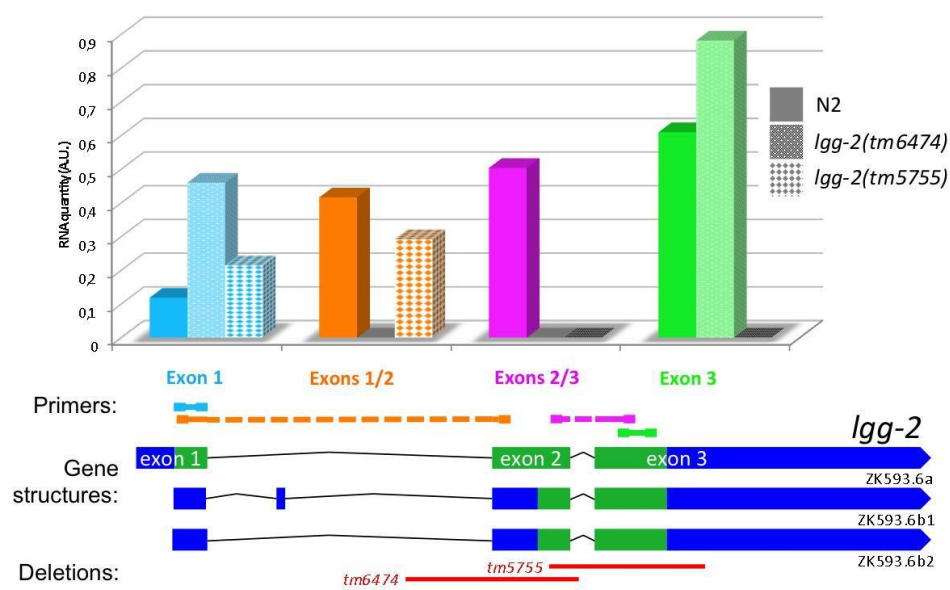
B

Figure S2: LGG-1-positive structures remain clustered in *lgg-2(tm5755)* as well as in *lgg-2(tm6474)* mutant embryos

A- *lgg-2* is transcribed from various positions along the gene, even in the *lgg-2* mutants. Q-PCR primers have been designed in different positions along *lgg-2* gene structure, as well as across the sequences deleted in the two mutants. B- MIP of confocal images of wild-type (N2), *lgg-2(tm6474)* and *lgg-2(tm5755)* embryos at meiosis II, ProNuclei (PN) migration, anaphase, 2-cell and 4-cell stages stained for LGG-1 (green) and DNA (blue). Vesicle-like structures labeled with LGG-1 (arrow heads) remain visible in both *lgg-2(tm5755)* and *lgg-2(tm6474)* at 4-cell stage. Insets on the right of each image are 4-fold magnified views of the highlighted areas. Dotted lines outline the embryos. Scale bar =10μm.
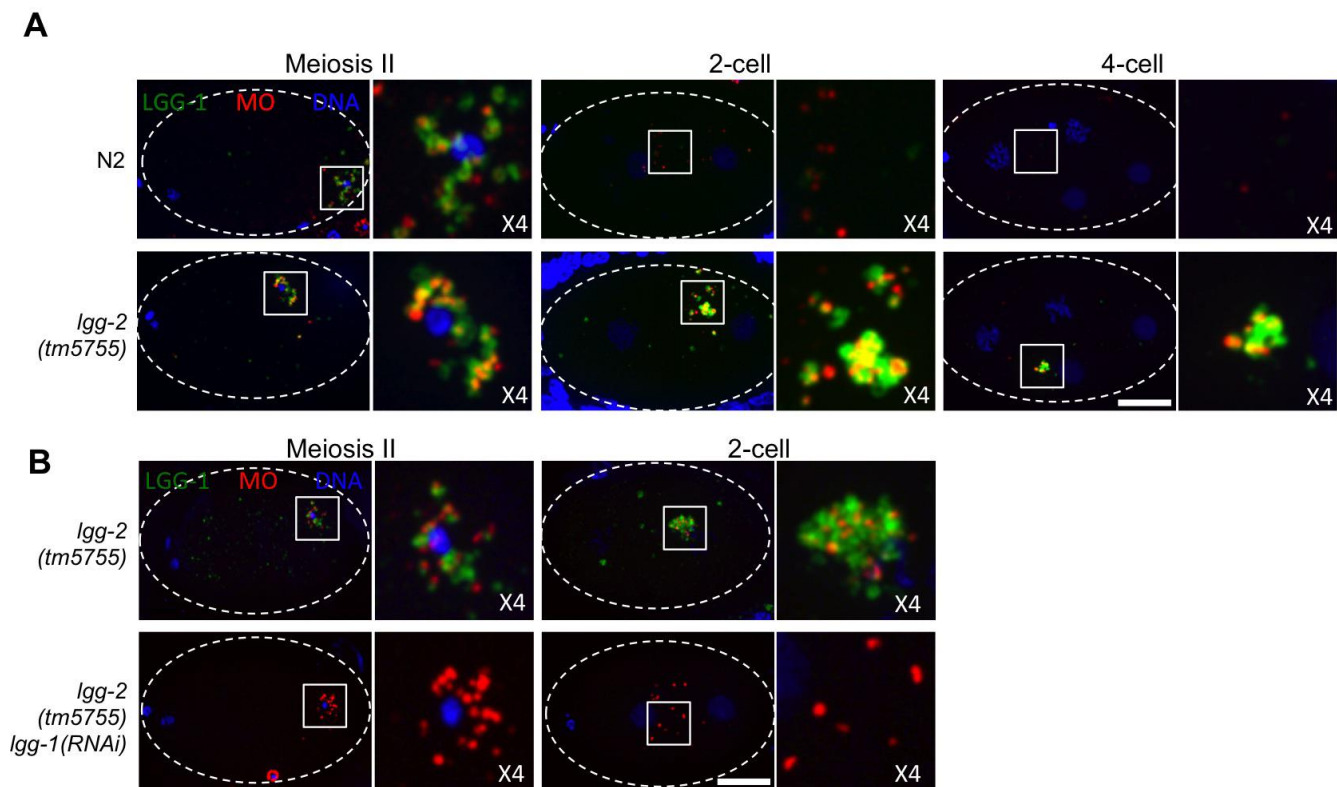
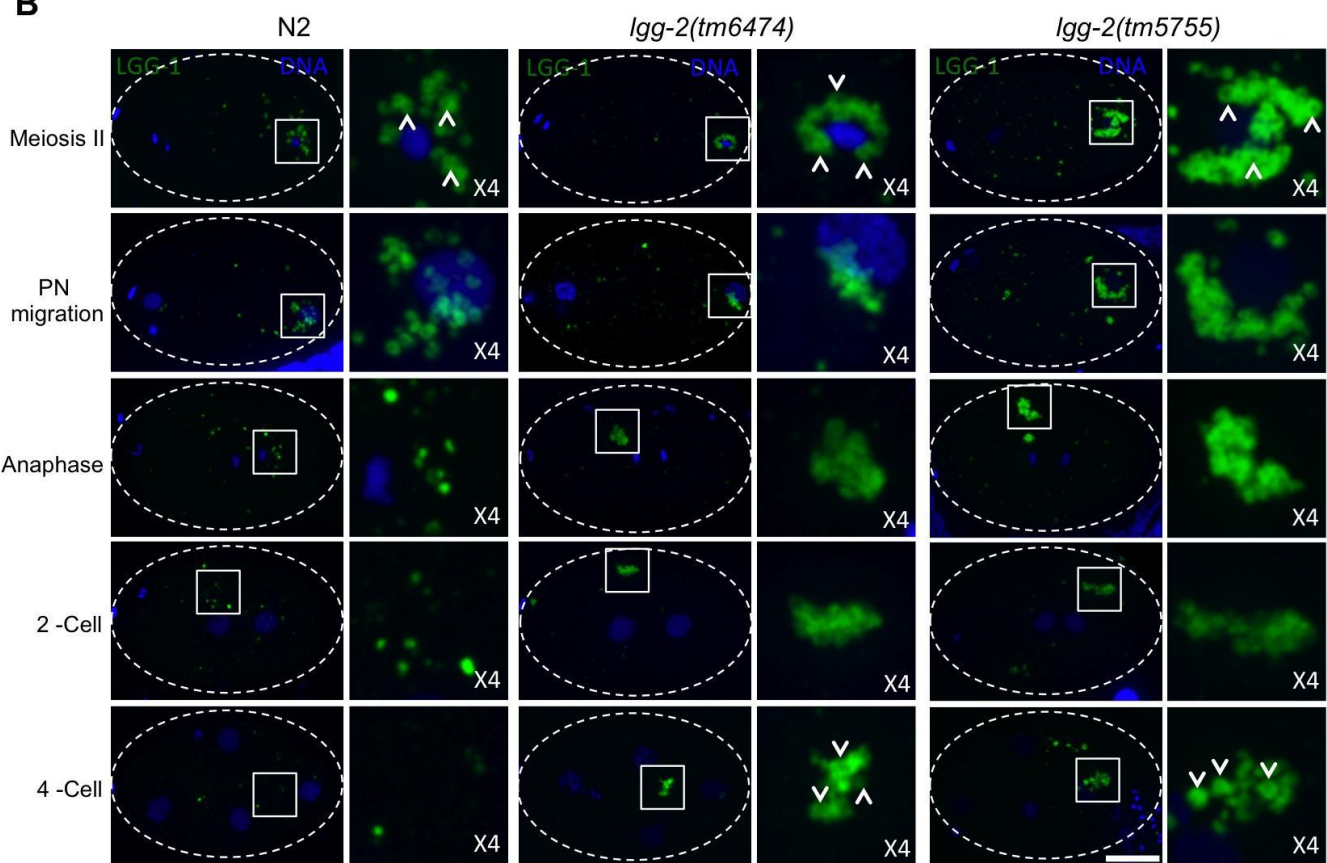**Figure S3:** LGG-1-positive structures and membranous organelles remain clustered in the absence of LGG-2

A- MIP of confocal images of wild-type (N2, upper panels) and *lgg-2(tm5755)* (lower panels) embryos at meiosis II, 2-cell and 4-cell stages, stained for LGG-1 (green), membranous organelles (red) and DNA (blue). B- MIP of confocal images of *lgg-2(tm5755)* (upper panels) and *lgg-2(tm5755); lgg-1(RNAi)* (lower panels) embryos at meiosis II and 2-cell stages stained for LGG-1 (green), membranous organelles (red) and DNA (blue). Insets on the right of each image are 4-fold magnified views of the highlighted areas. Dotted lines outline the embryos. Scale bars =10μm.
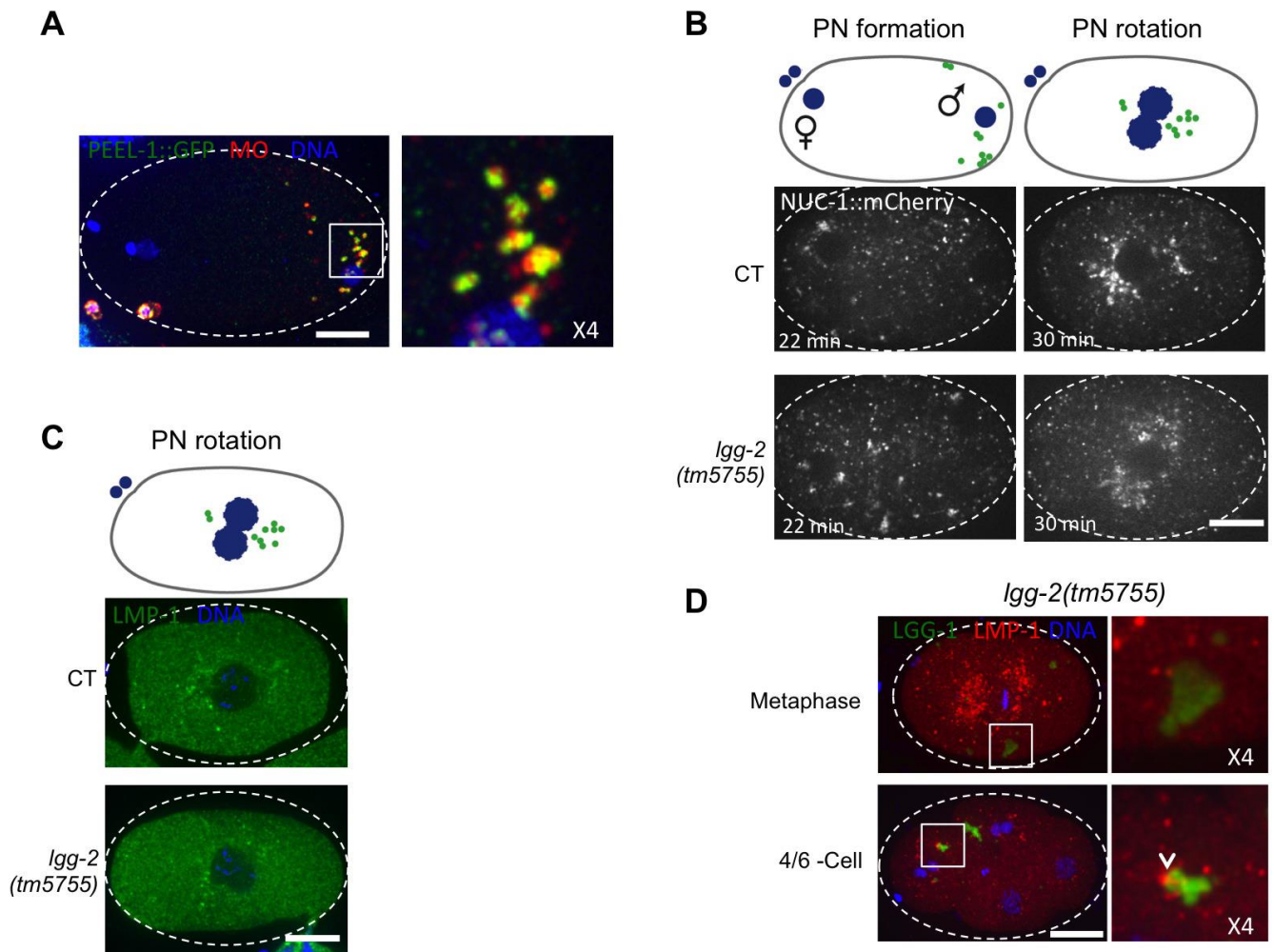
Figure S4: PEEL-1::GFP label the membranous organelles allowing their visualization after fertilization and the lysosomal markers NUC-1::mCHERRY and LMP-1 are enriched around centrosomes.

A- MIP of confocal images of an embryo fertilized by a spermatozoon expressing PEEL-1::GFP and stained for GFP (green), Membranous organelles (MO, red) and DNA (blue). Inset around sperm DNA is magnified 4-fold. Dotted lines outline the embryos. Scale bars=10μm. B- Schematic representation and still images from time-lapse recordings (single plane) of wild-type (CT, upper panels) and *lgg-2(tm5755)* (lower panels) embryos expressing the mCHERRY-tagged lysosomal nuclease (NUC-1::mCHERRY, gray) showing the distribution of lysosomes at ProNuclei (PN) formation and PN rotation stages (see Movie 6). C- Schematic representation and Maximum intensity Z-projections of immunofluorescence images of wild-type (N2, upper panels) and *lgg-2(tm5755)* embryos (lower panels) at pronuclei rotation stage, stained for LMP-1(green), and DNA (blue). Scale bars=10μm. D- MIP of confocal images of *lgg-2(tm5755)* embryos in metaphase and at the 4/6-cell stage and stained for LGG-1 (green), LMP-1 (red) and DNA (blue). The arrowhead indicates partial colocalization of LMP-1 and LGG-1 in the 4/6-cell stage embryo. Inset around clustered allophagosomes is magnified 4-fold. Scale bars =10μm.

Table 1: Primer list

The quantitative RT-PCR analysis of *lgg-2* RNAs were done using these primer pairs:

ama-1 : CCTACGATGTATCGAGGCAAA/CCTCCCTCCGGTGTAATAATG
(Hoogewijs et al., 2008)

lgg-2_Exon-1: GAGCGGAAATCGGGGAGGAT / GGAATGGCCTTCTTTCCTTGA

lgg-2_Exons-1/2 : CGGAAATCGGGGAGGATCTT / GTTGGCTGCGGATTTCTTCC

lgg-2_Exons-2/3 : ATAACCGTTGCCGAGCTCAT / TGAGCGTTCATTGACGAGCA

lgg-2_Exon-3 : AGCATTCTTCCTGCTCGTCA / GCCATCTGGATCACGCTCTT

The genotyping of the *lgg-2(tm5755)* and *lgg-2(tm6474)* strains was done using these primer pairs:

lgg-2(tm5755): GAGACTAGCCAAGTACACAG / CAAATTCCTAGTACCCGAGC

lgg-2(tm6474): TCAGAGACGCAGAGGACAGA/GGAGGCTGAAAAGCAAACGG

Table 2: Primary/secondary antibodies

	Host	Dilution	From	Reference
Anti-LGG-1	Rabbit	1/100	V. Galy	Al Rawi et al., 2011
Anti-LGG-1	Mouse	1/250	Gift from H. Zhang	
Anti-LGG-2	Rabbit	1/100	V. Galy	Al Rawi et al., 2011
Anti-RAB-5	Rabbit	1/250	Gift from A. Spang	Poteryaev et al., 2007
Anti-RAB-7	Rabbit	1/250	Gift from A. Spang	Poteryaev et al., 2007
Anti-MO	Mouse	1/500	Gift from S. Strome	Ward et al., 1986
Anti-tubulin	Mouse	1/1000	Sigma-Aldrich	T6199
Anti-tubulin	Rabbit	1/600	Abcam	ab18251
Anti-LMP-1	Mouse	1/10	Dev. Studies Hybridoma Bank	Hadwiger et al., 2010
Alexa-Fuor-488/anti-rabbit	Goat	1/800	Invitrogen	
Alexa-Fuor-488/anti-mouse	Goat	1/800	Invitrogen	
Alexa-Fuor-568/anti-rabbit	Goat	1/800	Invitrogen	
Alexa-Fuor-568/anti-mouse	Goat	1/800	Invitrogen	

Supplementary materials and methods

C. elegans strains and RNAi

Nematode strains were grown and handled as described (Brenner, 1974). Strains carrying the following mutations *lgg-2(tm5755)*, *lgg-2(tm6474)* were obtained from the National BioResource Project for the Nematode, *lgg-1(tm3489)* (Alberti et al., 2010) and *atg-3(bp412)* from the *Caenorhabditis elegans* Genetic Center. *lgg-2(tm5755)* mutant was backcrossed to wild-type twice prior to our analyses. *lgg-2(tm5755)* and *lgg-2(*tm6474) mutations were tracked using PCR genotyping using the primers presented in the supplementary material. The following strains are used in this study: transgenic strain expressing GFP::histoneH2B and GFP::β-Tubulin in the wild-type (XA3501, (Askjaer et al., 2002)) or in the *lgg-2(tm5755)* (VIG14, this study) backgrounds. Strain expressing LGG-2 under its endogenous promoter: *lgg-2::GFP::*LGG-2 (VIG06, (Al Rawi et al., 2011)) and *pie-1::GFP::tbg-1* (JUD209, generously provided by J. Dumont) were used for live imaging. Lysosomes were visualized using *ced-1::nuc-1::mCherry* transgenic worms in the wild-type (Liu et al., 2012) and in the *lgg-2(tm5755)* (VIG13, this study) backgrounds. Membranous organelles were visualized using *peel-1::peel-1::GFP* transgenic worms (EG5767, (Seidel et al., 2011)). The transgenic strain expressing GFP::LGG-1 in the germline (VIG19) was obtained by the MosSci technique using a recombination template generated by three-way gateway cloning technique in the destination vector pCFJ150 for recombination at the ttTi5605 mos1 insertion site (chromosome II). The 5' entry vector pJA254, containing the germline *mex-5* promotor and the

GFP-S65C, the middle entry vector containing full length synthetic *lgg-1* gene with intron and the 3' entry vector pCM1.36 containing the 3' UTR of *tbb-2 g*ene were used in the LR reaction with the pCFJ150 to generate the pVIG58 MosSci vector. The transgenic strain VIG19 was backcrossed twice before use. VIG20 was obtained by the cross of VIG19 with the *lgg-2(tm5755)* strain.

Bacterial clones from the J. Ahringer library (*atg-7*, *dhc-1*, *lgg-1*, *rab-5*, *rab-7* and empty vector L4440 for control) were used for RNAi "feeding" experiments (Kamath et al., 2003) as previously described (Al Rawi et al., 2011) except for *atg-5(RNAi),* which was done for two generations.

Quantitative RT-PCR:

The quantitative RT-PCR analysis was done on total RNA extracts of N2, *lgg-2(tm6474)* and *lgg-2(tm5755)* adult worms obtained using TRI Reagent, (SIGMA T9424). Reverse transcription on 1μg of RNA has been performed (Promega, A5002), and Q-PCR was carried out on a BioRad system (CFX 96 Real-Time) using the Evagreen dye (BIORAD 172-5211) and the primers listed in supplementary table 1.

Immunofluorescence staining and antibodies

C. elegans embryos immunostainings were performed as previously described (Galy et al., 2003) except for LMP-1 (Miller and Shakes, 1995) with the following modifications: the fixation was done at -80°C in methanol for 1 hour then in acetone for 30 minutes followed by a serial rehydration at room temperature in 75%, 50%, 25%, and 0% methanol in TBS (100mM NaCl, 50mM Tris-HCl, pH7.5). The primary antibodies used are listed in supplementary table 2.

Fluorescence imaging

The live imaging of the embryos mounted in meiosis buffer on agarose pads was done as described (Askjaer et al., 2014) on a Spinning Disk confocal microscope (Roper Scientific). Time-lapse images were acquired at 60sec intervals (except when specified). The imaging of fixed embryos was done as Z-stacks of images on the same Spinning Disk confocal microscope except for figure 3C: the deconvoluted images were obtained using a Delta-vision Core microscope. Image processing was done using the ImageJ software.

The quantitation of the fluorescence intensity of MO and sperm-mitochondria signals was done on Z-stacks of images from randomly selected embryos at the given stage of development defined by counting the number of DAPI stained nuclei. Images were acquired on a confocal Spinning Disk microscope as 76 pictures stacks every 0.4μm. The quantifications were done using image-J. The outer limit of each embryo was defined manually and for each pictures of the stack, the total signal intensity was measured in the region of interest defined as all the pixels of intensity above a fixed threshold. For each embryo, the total intensity was calculated as the sum of the total intensity measured in each plane. For each category the mean intensity was calculated and normalized to the mean intensity measured in meiosis embryos. Statistical analyses were conducted

with GraphPad Prism 5 software. Data were analyzed using Mann-Whitney non-parametric U test with $P < 0.05$ considered as significant.

The quantitation of the fluorescence intensity of GFP::LGG-1 in the 1 cell-stage embryos was done on Z-stacks extracted from time lapse recordings acquired on a confocal Spinning Disk microscope as 21 pictures stacks every 1μm. The quantifications were done using image-J. For each embryo, sum intensity projection was obtained. The outer limit of the embryo was defined manually and the average signal intensity was measured and normalized to the average signal intensity of the background.

Transmission electron microscopy

Transmission electron microscopy analysis was performed as previously described (Al Rawi et al., 2011) with the following modifications. After Epon infiltration, the samples were first polymerized as flat embedded blocks and observed on a DIC microscope to select one embryo of interest prior re-inclusion for serial sectioning. Thin sections were cut with an Ultracut UCT microtome (Leica) and were collected on 50 mesh formvar coated copper grids and poststained with 4% uranylacetate and Reynold's lead citrate. Images were taken with a Jeol 1010 at 80kV and equipped with a KeenView camera (Soft imaging systems).